Advanced Physical Research
Vol.4, No.3, 2022, pp.123-133

ADSORPTION OF ETHANOL BY FeO_2 CLUSTERS: TRANSITION STATE THEORY AND SENSING ANALYSIS

M.A. Abdulsattar[1,2*], H.M. Abduljalil[3], H.H. Abed[3]

[1]Department of Pharmacy, Al-Rasheed University College, Baghdad, Iraq
[2]Ministry of Science and Technology, Baghdad, Iraq
[3]Department of Physics, College of Science, University of Babylon, Iraq

Abstract. FeO_2 cluster adsorption and reaction with ethanol (C_2H_6O) using transition state theory are performed by density functional theory. First, the FeO_2 small clusters are proven to be thermodynamically more stable stoichiometry over Fe_2O_3 in normal temperature and pressure, as expected previously in the literature. The shallow ethanol transition state of -0.0123 eV is found on the FeO_2 surface compared to the adsorption and reaction energies at -1.154 and -7.8 eV, respectively. Reactions of ethanol with oxygen in the air are also considered. The maximum response temperature is at 280 ℃, so it is prior to the autoignition temperature of ethanol at 368.8 ℃. The variation of response with ethanol concentration is compared with the experiment. Response and recovery times are also calculated and compared with available experimental results.

Keywords: *Transition state theory, gas Sensor, ethanol detection, density functional theory.*

Corresponding Author: *M.A. Abdulsattar, Department of Pharmacy, Al-Rasheed University College, Baghdad, Iraq, e-mail: mudarahmed3@yahoo.com*

Received: *13 November 2022;* ***Accepted:*** *21 December 2022;* ***Published:*** *30 December 2022.*

1. Introduction

FeO_2 bulk structures are usually found at high pressure only (Gu & Liu, 2022; Koemets *et al*., 2021). However, recent experimental investigations found that FeO_2 can be found on Fe_2O_3 surfaces at normal pressure and temperature (Redondo *et al*., 2019). This can be explained by the fact that to reach equilibrium with the oxygen in the air, more oxygen atoms are attached to the surface of Fe_2O_3, making the stoichiometry of Fe_2O_3 crystals or particles shifts to FeO_2 at the surface. This is confirmed theoretically by density functional calculations (DFT) that show, at normal pressure and temperature, the clusters of ferric oxide (Fe_2O_3) react with extra oxygen atoms to become FeO_2 (Yu *et al*., 2018).

Many metal oxide materials are used as sensors, such as SnO_2 (Abdulsattar *et al*., 2021a), WO_3 (Zhao *et al*., 2022), ZnO (Abdulsattar *et al*., 2021b), Fe_2O_3 (Lei *et al*., 2023), etc. Nitrides and sulfides such as GaN (Li *et al*., 2022) and MoS_2 (Yoo *et al*., 2022) are also used as sensors. Other materials, such as graphene or reduced graphene oxide, are also used as sensors (Abdulradha *et al*., 2022). The interaction or reaction between the sensor material and the gas molecules can be either by physical adsorption (physisorption) or

How to cite (APA): Abdulsattar, M.A., Abduljalil, H.M., & Abed H.H. (2022). Adsorption of ethanol by FeO_2 clusters: Transition state theory and sensing analysis. *Advanced Physical Research, 4*(3), 123-133.

chemical reaction (chemisorption). The criteria for the adsorption to occur are the values of the thermodynamic energies, particularly Gibbs free energy. If the value of the Gibbs free energy is negative, the adsorption will proceed.

In order to calculate the value of Gibbs free energy, density functional theory (DFT) is used. The adsorption rate can be calculated using transition state theory (TST) (Abdulsattar, 2020). In TST, a transition state that controls the reaction rate must be overcome before the reaction can be completed. Several corrections are added to DFT calculations that are compatible with the nature of the adsorption process, such as dispersion corrections that consider the long-range forces in the adsorption process.

Ethanol is an important compound that has many applications, such as antiseptic and solvent for many materials (Maryam *et al*., 2021). The increasing amount of ethanol in human can lead to human body toxicity (Zink *et al*., 2020). Many materials are used to detect ethanol, such as SnO_2 and In_2O_3 (Son *et al*., 2022; Song *et al*., 2022). In the sensing mechanism of ethanol, ethanol can be either physisorbed or chemisorbed to the sensing material. The result is a change in the resistance of the adsorbing material that can indicate the existence of ethanol in the air surrounding the sensing material.

In the present work, the adsorption and detection of ethanol by FeO_2 oxide that exists as small clusters or on the surfaces of Fe_2O_3 bulk is discussed. The reaction rate of ethanol with FeO_2 is calculated using TST. The results of the reaction rate led to calculating the response, response time, and recovery time with both temperature and ethanol concentration. The theoretical results are compared with available experimental findings.

2. Theory

The oxidation states of iron have a wide range of oxides. However, the bulk oxides that mostly exist in nature are ferrous oxide (FeO), ferric oxide (Fe_2O_3), and magnetite (Fe_3O_4). Recent studies show that the surfaces of these oxides might have different stoichiometries because of exposure to oxygen in the air. As an example, FeO_2 can be found on Fe_2O_3 surfaces at normal pressure and temperature (Redondo *et al*., 2019). Small clusters of iron oxides at normal temperatures and pressure have also the preferred stoichiometry FeO_2 (Yu *et al*., 2018). This can be proved using thermodynamic quantities such as Gibbs free energy by using density functional theory. As an example, the Fe_8O_{12} cluster (with Fe_2O_3 stoichiometry) suggested by reference (Erlebach *et al*., 2015) (Fig. 1a) is thermodynamically unstable and transforms to FeO_2 stoichiometry (Fe_8O_{16}) as follows:

$$Fe_8O_{12}+2O_2 \rightarrow Fe_8O_{16}\ (\Delta G = -4.550\ \text{eV}), \quad (1)$$

$$Fe_8O_{16}+½O_2 \rightarrow Fe_8O_{17}\ (\Delta G = 0.797\ \text{eV}). \quad (2)$$

In the above equations, ΔG is the change in Gibbs free energy between products and reactants. The values of ΔG are obtained using the density functional theory at the level B3LYP/6-311G** (dispersion-corrected by GD3BJ version) that was tested several times for both cluster and gas sensor calculations (Mawwa *et al*., 2021; Muz & Kurban, 2022). B3LYP is a hybrid functional that incorporates some of the exact Hartree-Fock theory combined with empirical or theoretical exchange-correlation part. The name B3LYP is an abbreviation to (Becke, 3-parameter, Lee–Yang–Parr). The magnetization (spin) state of the clusters has only a small influence on their geometric structure (Erlebach *et al*., 2014).

As can be seen from Eq. (1) that the value of the change in Gibbs free energy is negative so that the reaction will continue forward until reaching equilibrium. The addition of oxygen to the initial stoichiometry Fe_8O_{12} is performed step by step, adding one oxygen atom at a time until reaching Fe_8O_{16}, which was all with negative Gibbs free energy. However, as Fe_8O_{16} be reached, the value of Gibbs free energy becomes positive, proofing that Fe_8O_{16} is the stable stoichiometry as in Eq. (2). This result leads to the fact that the different gases reactions at the surfaces of Fe_2O_3 bulk are actually with FeO_2 surfaces as mentioned earlier in the introduction part and previous references (Redondo *et al*., 2019; Yu *et al*., 2018).

The adsorption of ethanol at the Fe_8O_{16} cluster surface can be either by physisorption via van der Waals forces or chemisorption by oxygen reduction as in the following two equations:

$$Fe_8O_{16}+C_2H_6O\rightarrow[Fe_8O_{16}+C_2H_6O]^{ads}\ (\Delta G= -1.154\ eV), \quad (3)$$

$$6Fe_8O_{16}+C_2H_6O\rightarrow 6Fe_8O_{15}+2CO_2+3H_2O\ (\Delta G= -7.797\ eV). \quad (4)$$

As can be seen from Eqs. (3-4) that both physisorption and chemisorption are possible because of having negative Gibbs free energy. In order to calculate the adsorption rate of ethanol at the Fe_8O_{16} cluster surface, the transition state must be determined. The transition state is defined as the state with the highest potential energy along the reaction path. Gaussian 09 program (Frisch et al., 2013) is used to calculate the transition state:

$$Fe_8O_{16}+C_2H_6O\rightarrow[Fe_8O_{16}\text{---}C_2H_6O]^{\ddagger}\ (\Delta G^{\ddagger}= -0.0123\ eV), \quad (5)$$

$\Delta G^{\ddagger}$ is the Gibbs free energy of transition. The transition state $[Fe_8O_{16}\text{---}C_2H_6O]^{\ddagger}$ controls the reaction rate as in the following TST equation (Abdulsattar *et al*., 2021a; Abdulsattar *et al.*, 2021b):

$$\frac{d[Fe_8O_{16}]}{dt} = -A\ T\ [Fe_8O_{16}]\ [C_2H_6O]_e\ \exp^{\left(\frac{-\Delta G^{\ddagger}}{k_B T}\right)}. \quad (6)$$

In the above equation, $[Fe_8O_{16}]$ is the concentration of FeO_2 clusters, and $[C_2H_6O]_e$ is the effective concentration of ethanol. A in Eq. (6) is a pre-exponential factor, T is the temperature, and k_B is the Boltzmann constant. The use of effective concentration of ethanol is due to the burning of ethanol as temperature increases:

$$C_2H_6O+3O_2\rightarrow 2CO_2+3H_2O\ (\Delta G^{\ddagger}= -12.284\ eV). \quad (7)$$

The autoignition temperature of ethanol is 368.8℃ (Chen *et al*., 2010), after which ethanol burns rapidly. The distribution of ethanol due to its burning can be given by the logistic function:

$$f(T) = \frac{1}{1+e^{k(T-T_0)}} \quad (8)$$

In the above equation, k is the logistic growth, and T_0 is the 50% ethanol concentration temperature. The values of k and T_0 for ethanol that give the best fit to experimental results are 0.5 K^{-1} and 365 K, respectively.

Integrating Eq. (6), a 90% response time can be obtained (Abdulsattar *et al.*, 2021a; Abdulsattar *et al.*, 2021b; Abdulsattar *et al.*, 2021c):

$$t_{res(90\%)} = \frac{\ln(10)}{[C_2H_6O]_e \, A \, T \exp\left(\frac{-\Delta G^{\ddagger}}{k_B T}\right)} \tag{9}$$

Similarly, a 90% recovery time can also be obtained (Abdulsattar *et al.*, 2021a; Abdulsattar *et al.*, 2021b; Abdulsattar *et al.*, 2021c):

$$t_{rec(90\%)} = \frac{\ln(10)}{[O_2]_0 \, A \, T \exp\left(\frac{-\Delta G^{\ddagger}}{k_B T}\right)} + \sigma[C_2H_6O] \tag{10}$$

In the above equation, $[O_2]_0$ is the usual concentration of oxygen in the air. The effect of residual quantities of ethanol from the previous response phase is taken into account by the term $\sigma[C_2H_6O]$, where σ is an empirical parameter (Abdulsattar *et al.*, 2021a; Abdulsattar *et al.*, 2021b; Abdulsattar *et al.*, 2021c).

Sensor response is the resistance of the sensing material divided by the resistance when a specific concentration of ethanol is inserted (R_a/R_g). This ratio is proportional to the reaction rate of Eq. (6) (Abdulsattar *et al.*, 2021a; Abdulsattar *et al.*, 2021b):

$$\text{Response} = C \left|\frac{d[Fe_8O_{16}]}{dt}\right| + 1 \tag{11}$$

When the concentration of ethanol vanishes ($R_a = R_g$), the response is equal to 1, as in the above equation that corresponds to no reaction ($\frac{d[Fe_8O_{16}]}{dt} = 0$). C is the correlation parameter that has the value (475 s) in the present work that gives the best fit to available experimental values for FeO_2 sensitivity to ethanol (Mao et al., 2020).

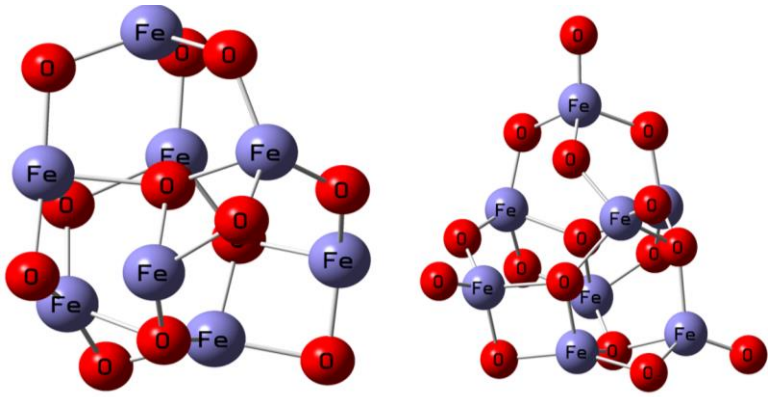

a) *b)*

Fig. 1. The two clusters (*a*) Fe_8O_{12} thermodynamically unstable cluster and (*b*) Fe_8O_{16} thermodynamically stable cluster in normal conditions (25 ℃ and 1 bar) after geometrical optimization. The Fe_8O_{12} cluster is suggested in reference (Erlebach *et al.*, 2015)

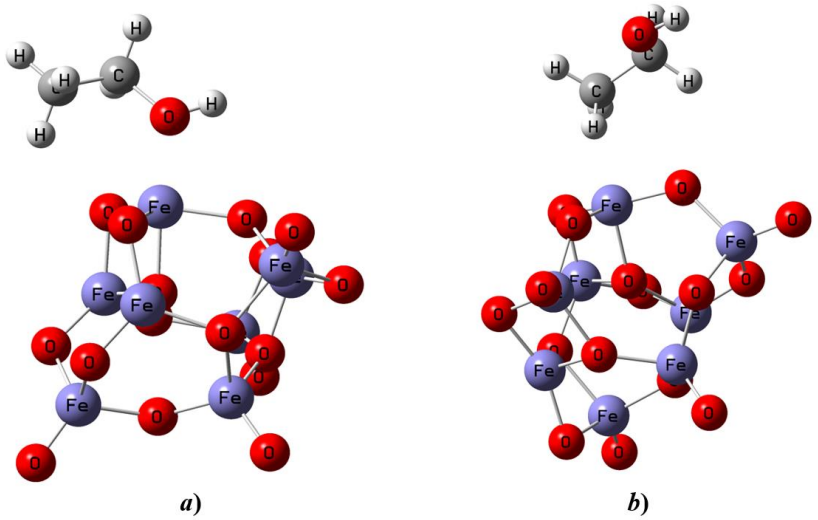

Fig. 2. (*a*) Adsorption state of ethanol on the Fe_8O_{16} cluster $[Fe_8O_{16}\text{---}C_2H_6O]^{ads}$, (*b*) transition state of ethanol on the Fe_8O_{16} cluster $[Fe_8O_{16}\text{---}C_2H_6O]^{‡}$.

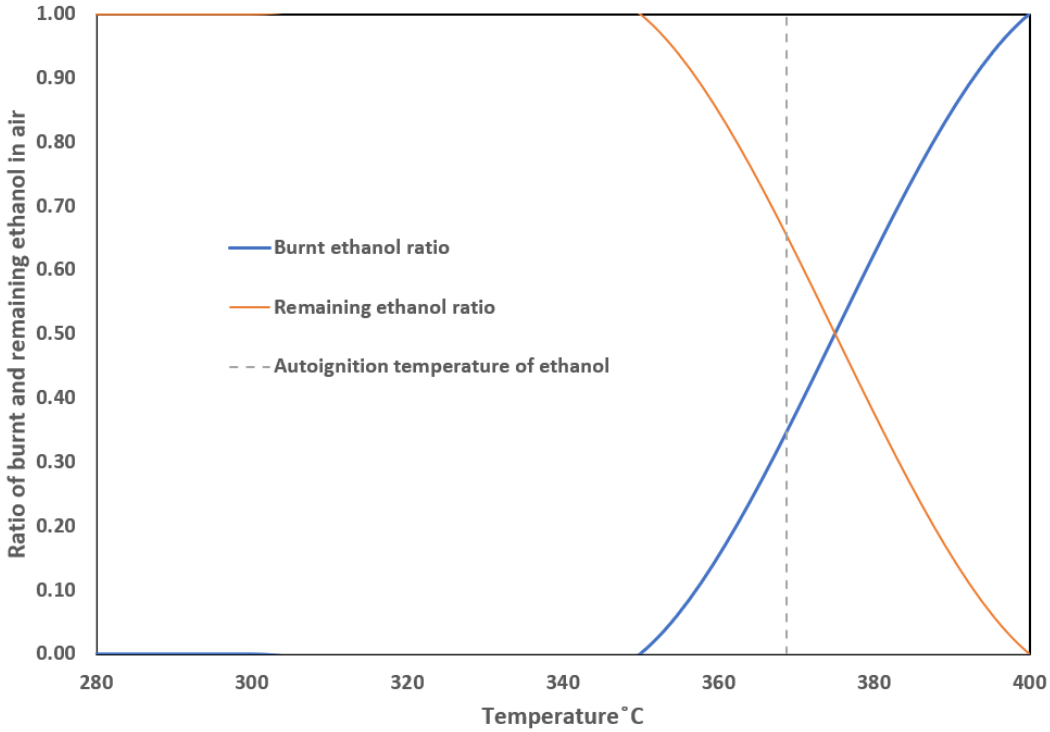

Fig. 3. Logistic function of the fraction of burning ethanol on Fe_8O_{16} cluster surface. The autoignition temperature and remaining fraction of ethanol is also shown.

3. Results and discussion

Fig. 4 shows the energy states diagram of the adsorption of ethanol on the surface of the Fe_8O_{16} cluster. The reaction rate is controlled by the slow transition between the initial state $Fe_8O_{16}+C_2H_6O$ to the transition state $[Fe_8O_{16}---C_2H_6O]^{‡}$ that has a small change in Gibbs free energy ($\Delta G^{‡}$= -0.0123 eV). The transition between the transition state $[Fe_8O_{16}---C_2H_6O]^{‡}$ to the final state $[Fe_8O_{16}---C_2H_6O]^{ads}$ is fast due to the high difference in the Gibbs free energy. This is also the case when a reaction proceeds, as in Eq. (4).

Fig. 5 shows the variation of response (R_a/R_g) of the Fe_8O_{16} cluster to ethanol as a function of temperature in comparison with the experiment. The highest response temperature is in good agreement with the experiment at nearly 280 °C (Mao *et al.*, 2020). The highest response value is also in good agreement with the experiment. The highest response temperature is usually less than the autoignition temperature of the sensed gas (Abdulsattar *et al.*, 2021a; Abdulsattar *et al.*, 2021c). However, the experimental values of response drop faster than the theory at low temperatures. The theoretical responses of high temperatures are in better agreement with experiments.

Fig. 6 shows the variation of response (R_a/R_g) of the Fe_8O_{16} cluster to ethanol as a function of ethanol concentration at maximum response temperature (280 °C) in comparison with the experiment. Good agreement can be seen in Fig. 6 between theory and experiment.

Fig. 7 and Fig. 8 show the variation of 90% theoretical response and recovery times with concentration of ethanol as described by Eq. (9) and Eq. (10), respectively, at a maximum response temperature of 280 °C. Despite the limited experimental values, a good agreement between theory and experiment can be seen. These figures can be used to extract response and recovery times for different ethanol concentrations.

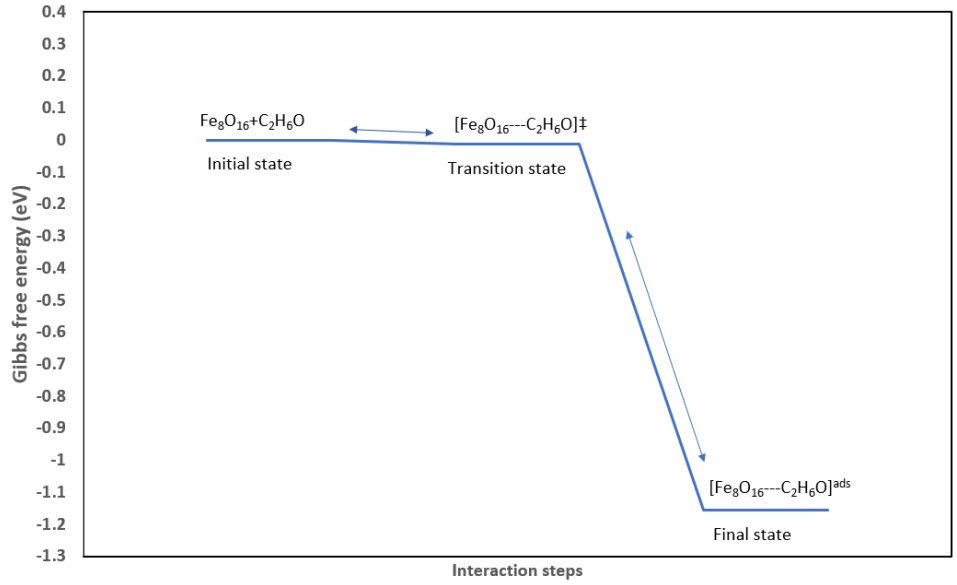

Fig. 4. The energy states of the reactants, transition state, and final state of ethanol on the Fe_8O_{16} cluster surface

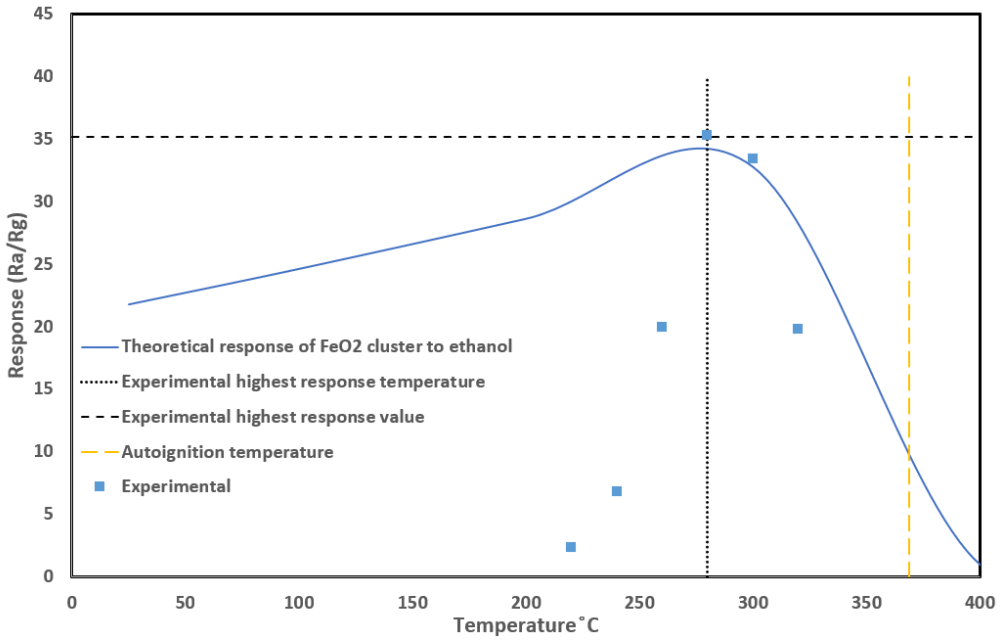

Fig. 5. Fe_8O_{16} cluster theoretical response to 100 ppm of ethanol as a function of temperature. Experimental results are from reference (Mao *et al.*, 2020)

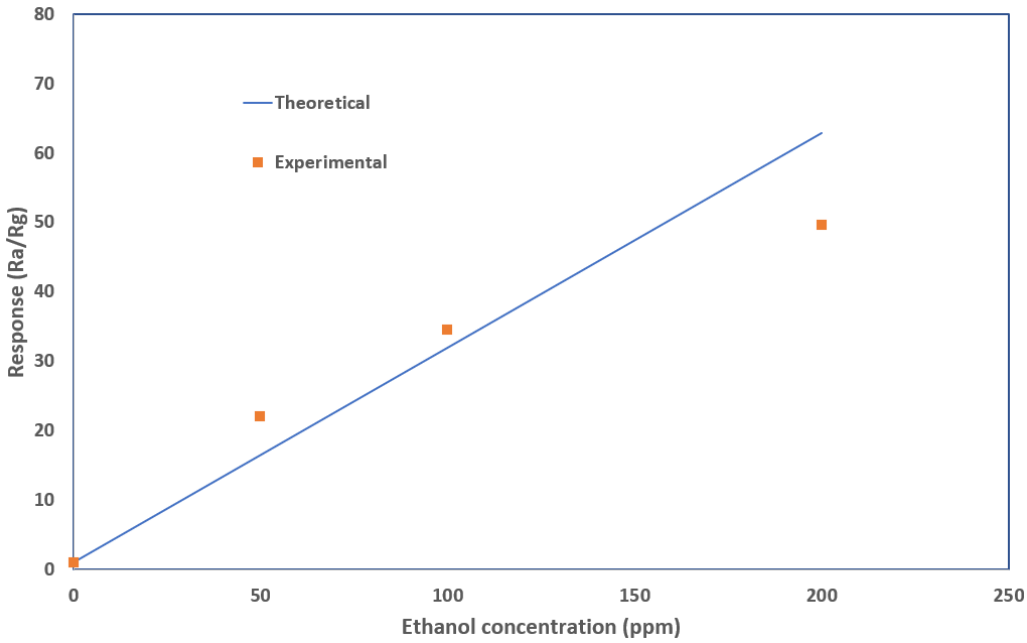

Fig. 6. Fe_8O_{16} cluster response to ethanol concentration at 280 °C. Experimental results are from reference (Mao *et al.*, 2020)

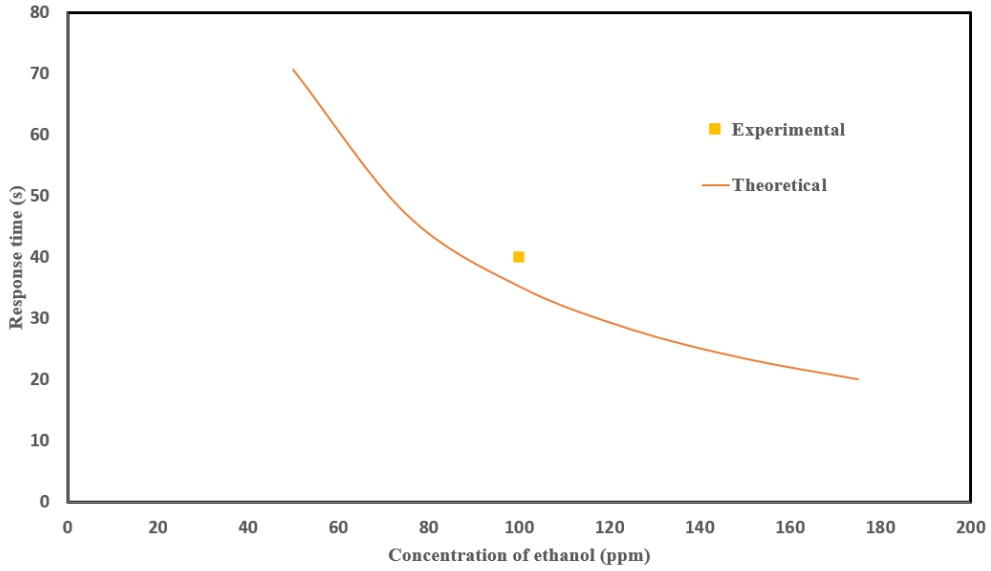

Fig. 7. Response time of Fe_8O_{16} cluster as a function of ethanol concentrations 280 °C. Experimental results are from reference (Mao *et al.*, 2020)

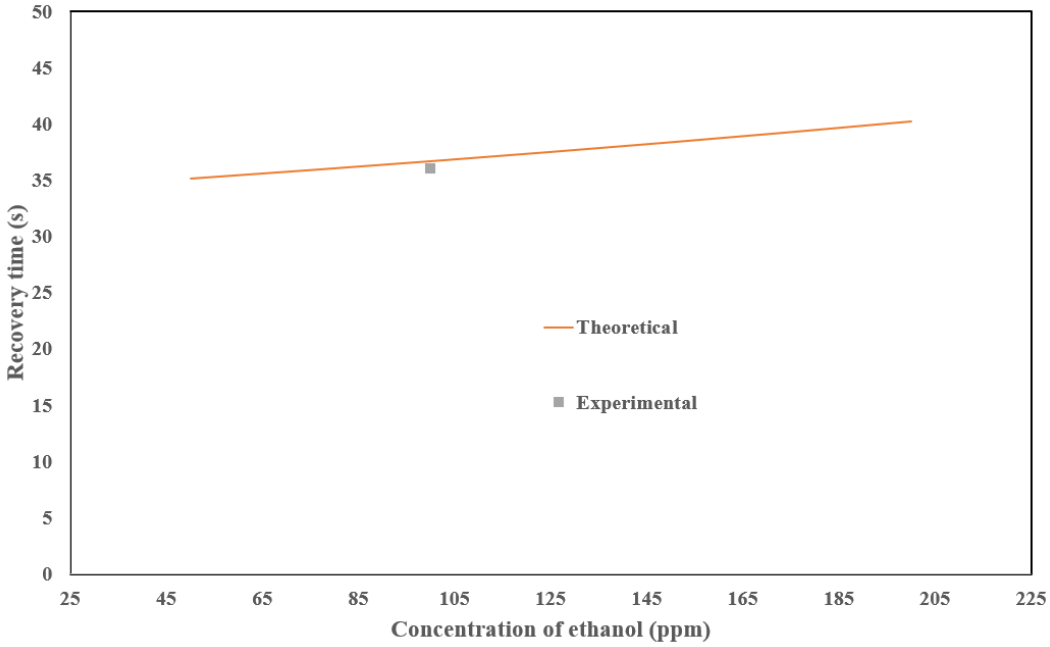

Fig. 8. Recovery time of Fe_8O_{16} cluster as a function of ethanol at 280 °C. Experimental results are from reference (Mao *et al.*, 2020)

Table 1 shows the parameters used in determining Figures (5-8). This includes the calculated Gibbs free energy of the transition state $\Delta G^{\ddagger}$, the reaction frequency parameter A, and the residual gas parameter σ. The calculated transition state energies have big differences between the response and recovery phases. The vanishing value of the response phase (-0.0123 eV) is contrasted by the high value of the recovery phase (1.142 eV). This

is the reverse situation for the frequency parameter A. The small value of A in the response phase (0.91 $(s.K)^{-1}$) is due to the small number of collisions of the gas that has a concentration in the range of ppm level. The high value of A in the recovery phase (15000000 $(s.K)^{-1}$) is due to the high number of collisions of oxygen atoms that forms one-fifth of all atoms in the usual atmosphere. The residual gas parameter exists only in the recovery phase. Its value (170 s) represents the time increment in the recovery phase due to the existence of residual ethanol gas (or other reaction product gases) that delays the restoration of full oxidized metal oxide.

Table 1. Transition state theory parameters needed to obtain theoretical results of response, response time, and recovery time. Note that $\Delta G^{\ddagger}$ is calculated using the present model while A and σ are fitting parameters that reflect the geometry of the sensor

No.	Reaction	A $(s.K)^{-1}$	$\Delta G^{\ddagger}$ (eV)	σ (s)
1	$Fe_8O_{16}+C_2H_6O \rightarrow [Fe_8O_{16}---C_2H_6O]^{\ddagger}$	0.91	-0.0123	-
2	$[Fe_8O_{16}---C_2H_6O]^{ads} \rightarrow [Fe_8O_{16}---C_2H_6O]^{\ddagger}$	15000000	1.142	170

4. Conclusions

FeO_2 is proved to be the stable thermodynamic stoichiometry for iron oxides in small clusters, which agrees with previous experimental and theoretical results. The transition state theory by its tool, namely density functional theory, is used to calculate the reaction rate of ethanol with FeO_2 cluster. Response of the cluster to ethanol as a function of temperature and ethanol concentration is in good agreement with the experiment except at low temperatures. 90% response and recovery times are also in good agreement with the experiment. The frequency parameter (A) and residual gas parameter (σ) are used to fit the theory results with the experiment. The value of the frequency parameter A is much smaller in the response phase than its value in the recovery phase, as expected from the number of collisions of the ethanol molecules in the response phase and the number of collisions of oxygen atoms in the recovery phase. The burning of ethanol due to reaching close to its autoignition temperature is considered.

References

Abdulsattar, M.A., Abed, H.H., Jabbar, R.H., & Almaroof, N.M. (2021a). Effect of formaldehyde properties on SnO2 clusters gas sensitivity: A DFT study. *Journal of Molecular Graphics and Modelling, 102*. https://doi.org/10.1016/j.jmgm.2020.107791

Abdulsattar, M.A., Jabbar, R.H., Abed, H.H., Abduljalil, H.M. (2021b). The sensitivity of pristine and Pt doped ZnO nanoclusters to NH3 gas: A transition state theory study. *Optik*, 242, 167158. https://doi.org/10.1016/j.ijleo.2021.167158

Abdulsattar, M.A., Jabbar, R.H., Abed, H.H. (2021c). Transition state application to simulate CO gas sensor of pristine and Pt doped tin dioxide clusters. *Journal of Physics: Conference Series*, *1963*(1), 012033. https://doi.org/10.1088/1742-6596/1963/1/012033

Abdulradha, S.K., Hussein, M.T., Abdulsattar, M.A. (2022). Study of the interaction between reduced graphene oxide and NO_2 gas molecules via Density Functional Theory (DFT). *International Journal of Nanoscience*, *21*(2), 2250009. https://doi.org/10.1142/S0219581X22500090

Abdulsattar, M.A. (2020). Transition state theory application to H_2 gas sensitivity of pristine and Pd doped SnO2 clusters. *Karbala International Journal of Modern Science*, *6*(2), 13(205-

214). https://doi.org/10.33640/2405-609X.1615

Chen, C.-C., Liaw, H.-J., Shu, C.-M., Hsieh, Y.-C. (2010). Autoignition temperature data for methanol, ethanol, propanol, 2-butanol, 1-butanol, and 2-methyl-2,4-pentanediol. *Journal of Chemical and Engineering Data*, *55*(11), 5059-5064. https://doi.org/10.1021/je100619p

Erlebach, A., Hühn, C., Jana, R., Sierka, M. (2014). Structure and magnetic properties of $(Fe_2O_3)n$ clusters (n = 1-5). *Physical Chemistry Chemical Physics*, *16*(48), 26421-26426. https://doi.org/10.1039/c4cp02099e

Erlebach, A., Kurland, H.-D., Grabow, J., Müller, F. A., Sierka, M. (2015). Structure evolution of nanoparticulate Fe_2O_3. *Nanoscale*, *7*(7), 2960-2969. https://doi.org/10.1039/c4nr06989g

Frisch, M.J., Trucks, G.W., Schlegel, HB., Scuseria, G.E., Robb, M.A., Cheeseman, J.R., Scalmani, G., Barone, V., Mennucci, B., Petersson, G.A., Nakatsuji, H., Caricato, M., Li, X., Hratchian, H.P., Izmaylov, A.F., Bloino, J., Zheng, G., Sonnenberg, J.L., Hada, M., … Fox, D. J. (2013). *Gaussian 09, Revision D.01*. Gaussian, Inc.

Gu, X., Liu, L. (2022). First-Principles Calculation on Crystal Structure and Elastic Properties of Py-FeO_2, Py-FeOOH and ε-FeOOH under High Pressures. *Gaoya Wuli Xuebao/Chinese Journal of High Pressure Physics*, *36*(1). https://doi.org/10.11858/gywlxb.20210789

Koemets, E., Leonov, I., Bykov, M., Bykova, E., Chariton, S., Aprilis, G., Fedotenko, T., Clément, S., Rouquette, J., Haines, J., Dubrovinskaia, N., Dubrovinsky, L. (2021). Revealing the complex nature of bonding in the binary high-pressure compound FeO_2. *Physical Review Letters*, *126*(10), 106001. https://doi.org/10.1103/PhysRevLett.126.106001

Lei, Z., Cheng, P., Wang, Y., Xu, L., Lv, L., Li, X., Sun, S., Hao, X., Zhang, Y., Zhang, Y., Zhang, Y., & Weng, Z. (2023). Pt-doped α-Fe_2O_3 mesoporous microspheres with low-temperature ultra-sensitive properties for gas sensors in diabetes detection. *Applied Surface Science*, 607, 154558. https://doi.org/10.1016/j.apsusc.2022.154558

Li, D., Han, D., Chen, Y., Liu, Z., Liu, X., Liu, L., Han, X., He, X., & Sang, S. (2022). Hollow porous GaN nanofibers gas sensor for superior stability and sub-ppb-level NO_2 gas detection. *Sensors and Actuators B: Chemical*, 371, 132583. https://doi.org/10.1016/j.snb.2022.132583

Mao, J.N., Hong, B., Chen, H.D., Gao, M.H., Xu, J.C., Han, Y.B., Yang, Y.T., Jin, H.X., Jin, D.F., Peng, X.L., Ge, H.L., Wang, X.Q. (2020). Highly improved ethanol gas response of n-type α-Fe_2O_3 bunched nanowires sensor with high-valence donor-doping. *Journal of Alloys and Compounds*, 827, 154248. https://doi.org/10.1016/j.jallcom.2020.154248

Maryam, S., Hartono, K., Widiyawati, I.E. (2021). Clove leaf ethanol extract (Syzygium aromaticum L. Merr. And Perr) is formulated as antiseptic liquid soap. *Journal of Physics: Conference Series*, *1869*(1), 012003. https://doi.org/10.1088/1742-6596/1869/1/012003

Mawwa, J., Shamim, S. U. D., Khanom, S., Hossain, M. K., & Ahmed, F. (2021). In-plane graphene/boron nitride heterostructures and their potential application as toxic gas sensors. *RSC Advances*, *11*(52), 32810-32823. https://doi.org/10.1039/d1ra06304a

Muz, I., Kurban, M. (2022). Zinc oxide nanoclusters and their potential application as CH_4 and CO_2 gas sensors: Insight from DFT and TD-DFT. *Journal of Computational Chemistry*, *43*(27), 1839-1847. https://doi.org/10.1002/jcc.26986

Redondo, J., Lazar, P., Procházka, P., Průša, S., Mallada, B., Cahlík, A., Lachnitt, J., Berger, J., Šmíd, B., Kormoš, L., Čechal, J., Švec, M. (2019). Identification of Two-Dimensional FeO2 Termination of Bulk Hematite α-Fe2O3(0001) Surface. *Journal of Physical Chemistry C*, *123*(23), 14312-14318. https://doi.org/10.1021/acs.jpcc.9b00244

Son, D.N., Hung, C.M., Thi Thanh, L.D., Thi Xuan, C., Van Duy, N., Dich, N.Q., Nguyen, H., Van Hieu, N., Hoa, N.D. (2022). A novel design and fabrication of self-heated In_2O_3 nanowire gas sensor on glass for ethanol detection. *Sensors and Actuators A: Physical*, 345, 113769. https://doi.org/10.1016/j.sna.2022.113769

Song, W., Zhang, M., Zhao, W., Zhao, Q., Hao, H., Lin, H., Gao, W., Yan, S. (2022). Nanostructured SnO_2 Microsphere-Based Gas Sensor Array Enhanced by Molecular Imprinting for Methanol and Ethanol Discriminative Detection. *ACS Applied Nano*

Materials, *5*(9), 12765-12777. https://doi.org/10.1021/acsanm.2c02662

Yoo, C., Yoon, J., Kaium, M. G., Osorto, B., Han, S. S., Kim, J. H., Kim, B. K., Chung, H.-S., Kim, D.-J., Jung, Y. (2022). Large-area vertically aligned 2D MoS_2 layers on TEMPO-cellulose nanofibers for biodegradable transient gas sensors. *Nanotechnology*, *33*(47), 475502. https://doi.org/10.1088/1361-6528/ac8811

Yu, X., Oganov, A. R., Zhu, Q., Qi, F., Qian, G. (2018). The stability and unexpected chemistry of oxide clusters. *Physical Chemistry Chemical Physics*, *20*(48), 30437-30444. https://doi.org/10.1039/c8cp03519a

Zhao, C., Shen, J., Xu, S., Wei, J., Liu, H., Xie, S., Pan, Y., Zhao, Y., Zhu, Y. (2022). Ultra-efficient trimethylamine gas sensor based on Au nanoparticles sensitized WO_3 nanosheets for rapid assessment of seafood freshness. *Food Chemistry*, 392, 133318. https://doi.org/10.1016/j.foodchem.2022.133318

Zink, A., Conrad, J., Telugu, N. S., Diecke, S., Heinz, A., Wanker, E., Priller, J., Prigione, A. (2020). Assessment of Ethanol-Induced Toxicity on iPSC-Derived Human Neurons Using a Novel High-Throughput Mitochondrial Neuronal Health (MNH) Assay. *Frontiers in Cell and Developmental Biology*, 8, 590540(1-20). https://doi.org/10.3389/fcell.2020.590540